*Aust. J. Phys.*, 1990, **43**, 683–702

# Spectroscopy and Structure of Aromatic–Rare Gas Cluster Ions*

*Ruth I. McKay, Evan J. Bieske,*[A] *Ian M. Atkinson, Frederick R. Bennett, Andrew J. Bradley, Mark W. Rainbird, Andrew B. Rock, Angelo S. Uichanco and Alan E. W. Knight*

Molecular Dynamics Laboratory, Division of Science and Technology, Griffith University, Brisbane, Qld 4111, Australia.
[A] Physikalisch-Chemisches Institut der Universitat Basel, Klingelbergstrasse 80, CH-4056 Basel, Switzerland.

*Abstract*

Ionic clusters consisting of a polyatomic ion surrounded by a few 'solvent' atoms or molecules, provide a connecting link between the isolated gas phase ion and the ion solvated in a condensed medium. Analysis of the vibrational structure associated with the motion of the cluster atoms can reveal details concerning the intermolecular potential. However, for large polyatomic ions, information concerning the cluster vibrational motion has been difficult to obtain using conventional spectroscopic methods. We have developed a new combination of the previously available techniques of supersonic cooling, resonance-enhanced multiphoton ionisation, time-of-flight mass spectroscopy, in concert with one-photon photodissociation spectroscopy. This new technique takes advantage of the facile predissociation of an electronically excited cluster and affords us a method of studying the previously unmeasurable vibrational structure associated with the motion of a molecular cluster ion. Using this technique we have obtained vibrationally resolved photodissociation spectra of a number of aromatic–rare gas cluster ions. Analysis of their vibrational structure permits structural details of the cluster cation to be deduced.

## 1. Introduction

Bimolecular collisions in the gas phase lead to either elastic, inelastic or reactive scattering. The dynamics of a molecular collision can be defined in terms of such quantities as impact parameters, relative kinetic energies and an interaction potential that in many cases may be determined with relatively high precision either experimentally using molecular beam scattering methods, or theoretically from *ab initio* calculations. The field is relatively mature, with an extensive literature covering both atomic and molecular systems and a wide variety of scattering processes.

Condensed phase interactions have received continuing attention for many decades, but the level of precision in both theory and experiment has often been far less than that available in the study of gas phase processes. In recent years, our understanding of the condensed phase has enjoyed an enormous boost through the discovery of new experimental methodologies such as scanning tunnelling microscopy (STM), ultrafast (femtosecond) laser

* Paper presented at the Workshop on Interfaces in Molecular, Electron and Surface Physics, held at Fremantle, Australia, 4–7 February 1990.

0004-9506/90/040683$03.00

spectroscopy and a large armory of surface analysis techniques, as well as the advent of supercomputers and associated development of theoretical methods.

Small clusters of atoms or molecules held together by weak intermolecular forces, occupy a class in nature that has been embraced as a 'fifth state' of matter with unique properties that permit the transition between gas and condensed phase properties to be subjected to controlled investigation. The reduced complexity of small clusters gives us a chance to attempt a detailed theoretical understanding of intermolecular forces and condensed phase behaviour. The wide interest in clusters (Blaney and Ewing 1976; Levy 1981; Castleman and Keesee 1986) has been stimulated in part by a desire to better understand the nature of the relatively weak bonding interactions that are normally associated with the adhesion of atoms and molecules to surfaces, or the interactions between solvent and solute. Clusters serve as prototypes for gas–surface interactions or solvation processes, but with the advantage, relative to the condensed phase, of offering the opportunity for measuring properties with a precision approaching that which is normally achievable for isolated gas phase species, as bulk effects are avoided.

Our own interest in cluster studies includes the exploration of ionic clusters, i.e. aggregates formed when ions adhere to atomic or molecular partners. Charged aggregates of atoms and molecules are ubiquitous in flames and other combustion processes, in the upper and lower atmosphere, in outer space, in effluent from nuclear fission reactors and fusion processes in plasmas, and in fact, wherever matter is exposed to ionising radiation. They are also central actors in electrolytic, solvation and nucleation processes. The net nonzero charge on a molecular ion means that at distances large enough for neutral molecules to have little influence on their neighbours, ions still exert polarising forces on their surrounding environment. Thus whenever present, molecular ions tend to dominate the chemical processes occurring in a system. Aside from the intrinsic interest in understanding the interaction between ions and neutral molecules, ionic clusters serve as a connecting link between the isolated gas phase ion and the ion solvated in a condensed medium (Castleman and Keesee 1986).

Molecular ions have often been elusive species with respect to experimental detection, e.g. the $H_3O^+$ cation was postulated in solution reaction mechanisms long before it was isolated experimentally. Ions are generally difficult to prepare nondestructively in sufficient isolable concentrations so as to facilitate detection and characterisation with standard spectroscopic tools, as they are prone to rapid reaction. Nevertheless, their study has been pursued with vigour for some time. Matrix isolation methods have been used to trap ions for investigation with photoelectron spectroscopy (Turner *et al.* 1970), IR and UV absorption spectroscopy (Friedman *et al.* 1984; Lurito and Andrews 1985) and laser spectroscopy (Maier and Marthaler 1978; Bondybey and Miller 1983; Maier 1986).

The advent of supersonic expansion cooled molecular beams has contributed spectacularly to the simplification of the spectroscopy of large polyatomic molecules, as well as providing a versatile means of synthesising and studying van der Waals complexes, radicals and molecular ions. The environment of a supersonic expansion, in which the clusters have very low internal energies and long collision-free lifetimes, enables weakly bonded clusters and transient

species, such as radicals and ions, to exist for experimentally observable lifetimes, and permits spectra to be measured without significant contribution from thermal inhomogeneous broadening. Laser-induced fluorescence spectroscopy (LIF) has been employed successfully to measure properties of ions prepared in supersonic free jet expansions (Heaven *et al.* 1982; DiMauro *et al.* 1984). The advantages of LIF over conventional absorption spectroscopy are that the spectral resolution is determined largely by the laser bandwidth rather than spectral slitwidth and that techniques such as two-photon excitation may be used to eliminate the Doppler width of spectral lines.

LIF techniques are only applicable for fluorescing species. Many polyatomic ions, especially those involving larger substituted aromatic rings, display low fluorescence quantum yields due to the existence of efficient non-radiative relaxation channels from the electronically excited state. Given that our interests lie in the larger polyatomics, we have been motivated to develop alternative techniques for obtaining high resolution spectroscopic information for these systems. Moreover, our prime goal is to seek information on ionic clusters. LIF suffers from the disadvantage that it does not provide a ready means of discriminating between the various different cluster species, A-$(M)_n$ ($n = 1, 2, 3...$), that are inevitably formed in a supersonic molecular expansion of polyatomic (A) in a carrier gas (M). LIF studies of cluster ions carried out so far (Kennedy and Miller 1986; Kung *et al.* 1988) have proven somewhat ambiguous due to overlapping contributions in the measured spectra due to the many cluster species present.

The strategy that we have chosen to pursue in the study of ionic clusters makes use of time-of-flight mass spectrometry (TOFMS) to separate the different cluster species by mass, thereby permitting each species to be studied selectively. We use tunable laser resonance-enhanced two-photon ionisation (R2PI) to prepare ions directly from their parent neutral clusters, thereby restricting the range of cluster ion species that are created. The cluster ions so prepared are rotationally cold ($\leq$10 K) and vibrational populations are significant only for a few of the lowest vibrational states. The excitation spectroscopy of these cluster ions is probed using a novel application of one-photon photodissociation spectroscopy. These combined methodologies have permitted us to obtain the first clear and unambiguous view of the extended vibrational structure associated with the low frequency motion of a rare gas atom against an aromatic cation (Bieske *et al.* 1990*a*, 1990*b*; McKay *et al.* 1990).

A typical vibrational mode of a polyatomic molecule has a vibrational frequency ranging from ~150–3000 $cm^{-1}$. The vibrational motions associated with a van der Waals bond are of a much lower frequency due to the much weaker nature of the bond. Transitions involving the low frequency van der Waals vibrations of a neutral rare gas–molecule complex, i.e. the symmetric bend, $b_x$, the asymmetric bend, $b_y$, and the symmetric stretch, $s_z$, have been documented in the recent literature (Brumbaugh *et al.* 1983; Boesiger and Leutwyler 1986; Butz *et al.* 1986; Menapace and Bernstein 1987; Jacobsen *et al.* 1988; Weber and Rice 1988*a*, 1988*b*, 1988*c*; Weber *et al.* 1988; Bieske *et al.* 1989*b*; Mons *et al.* 1989). We have shown recently (Bieske *et al.* 1989*b*) that the intensity profiles associated with the low frequency transitions in the electronic spectra of a range of aromatic–rare gas systems deviate substantially from those expected on the basis of harmonic vibrational overlap

integrals (Franck–Condon factors). A model involving stretch-bend anharmonic coupling via cubic and quartic terms in the intermolecular potential accounts satisfactorily for the observed spectral features (Bieske *et al.* 1989*b*; McKay *et al.* 1990). We anticipate that the interaction between the stretching and bending motions is a general property of clusters and we expect that it will also appear as an important consideration in the vibrational dynamics of cluster ions.

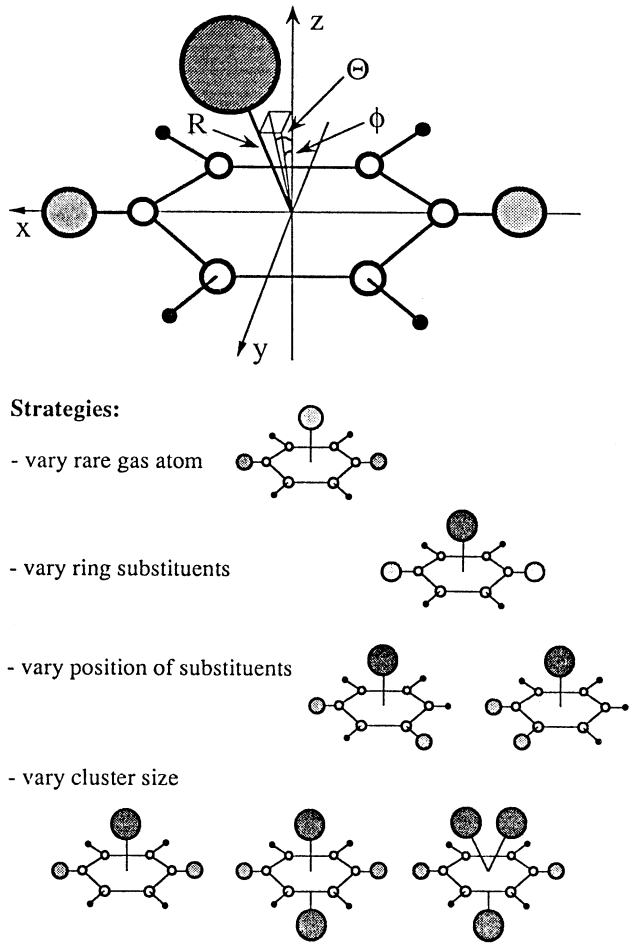


**Fig. 1.** Schematic showing the structure of the cluster ion formed between *p*-difluorobenzene$^+$ ($C_6H_4F_2$) and argon. The structural parameters $R$, $\theta$, $\phi$ are defined. Also illustrated are some of the experimental strategies that can be used to explore the structural and dynamical features of aromatic–rare gas cluster ions.

Fig. 1 illustrates a typical cluster ion formed when an argon atom binds to the polyatomic *para*-difluorobenzene$^+$ ($C_6H_4F_2^+$ or *p*DFB$^+$). Measurement of vibrationally and rotationally resolved electronic excitation spectra permit the structural details of the cluster ion to be determined (Yamanouchi *et al.* 1984, 1987). Spectroscopic data that permit the accurate construction of intermolecular potentials for solvated ions are rare. This is particularly so for

aromatic cations, where even vibrational information for the isolated cation is mostly unavailable. The structure of the ionic cluster can be characterised by the distance $R$ of the argon atom from the centre of mass of the aromatic molecule, and the angles $\theta$, $\phi$ relative to the normal to the aromatic ring plane. These three coordinates define the location of the argon atom above the plane of the aromatic ring. Using the approximation that the vibrational motion of the argon atom is decoupled from the much higher frequency motion of the atoms that constitute the $C_6H_4F_2$ ring, the vibrational dynamics of the cluster bond may be modelled by an intermolecular potential function $V(R, \theta, \phi)$. The validity of this approximation may be tested by comparing the experimental observables with theoretical predictions deduced from this simplified model.

A variety of experimental strategies may be used to refine the theoretical description of the atom–substrate interaction. Systematic variations can be made easily to test the ability of any intermolecular potential model to match observed experimental measurements. For example (see Fig. 1), the degree of clustering may be varied, both theoretically and experimentally, to test how the theoretical parameters respond to changes in the number of rare gas atoms bound to the aromatic substrate. The nature of the substituents on the aromatic ring can be varied (e.g. fluorobenzene to chlorobenzene), the relative positions of substituents on the aromatic can be varied to change the symmetry of the molecule (e.g. *para*-difluorobenzene to *meta*-difluorobenzene),

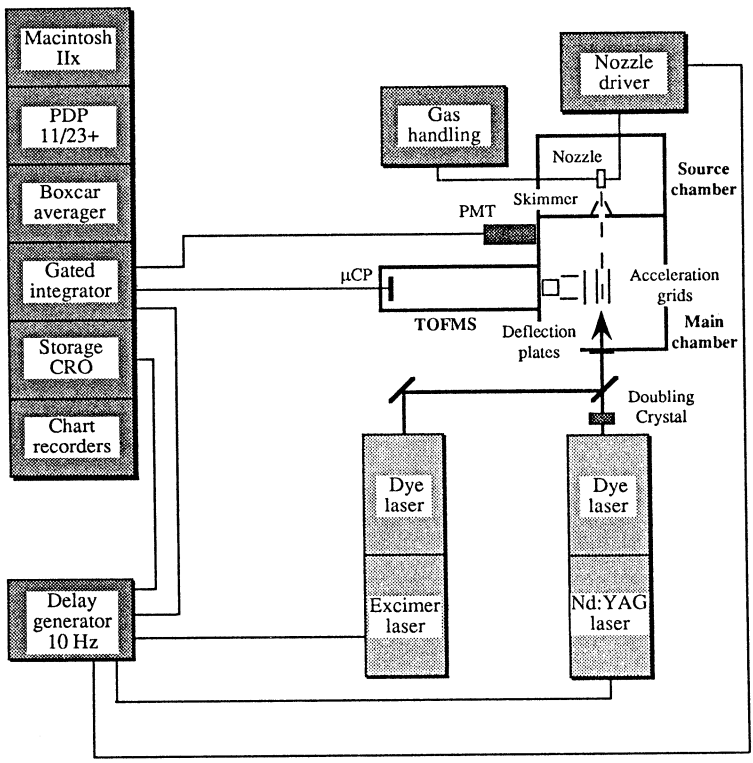


**Fig. 2.** Schematic showing the experimental configuration used.

or the identity of the rare gas atom may be varied (e.g. He, Ne, Ar, Kr, Xe). We may also examine the changes in the equilibrium structure ($\Delta R_0, \Delta\theta_0, \Delta\phi_0$) upon electronic excitation. A further issue that may be explored is whether three-body or higher order interactions are important. Further experimental directions may be concerned with observing the photoejected electron—its polarisation, kinetic energy and angle of ejection, perhaps measuring it in coincidence with its companion ion (known as PIPECO—photoion photoelectron coincidence).

## 2. Experimental Methods

Fig. 2 provides a schematic of the experimental apparatus used in our studies of ionic clusters. The main components of the vacuum chamber are (a) a source chamber where neutral van der Waals clusters are formed in a molecular beam expansion; (b) a main chamber where the skimmed molecular beam is directed through acceleration grids for ion deflection and where lasers intersecting the molecular beam are used both to ionise and to induce vibrationally resolved electronic state changes and photofragmentation and (c) a time-of-flight mass spectrometer that is used to mass selectively detect the laser prepared parent ions and photofragments. Tunable dye lasers (either Nd:YAG or excimer pumped, frequency doubled for ionisation laser) are used both to ionise the clusters, and to interrogate the resulting ions. Spectral data are collected and stored on a PDP 11/23+ and downloaded for analysis on a Macintosh IIx. Lasers, nozzle and detection apparatus are triggered at 10 Hz using a home built programmable delay generator. Various aspects of the experimental methodology are described below.

### *(a) Cooling in Supersonic Expansions*

Clusters formed by the association of neutral polyatomic molecules with rare gas atoms may be generated readily by expanding a small concentration (typically 1%) of the molecular species together with the atomic carrier gas through a nozzle orifice (typically 1mm diam.) into a chamber evacuated to a pressure of $\leq 10^{-4}$ Torr ($\equiv 0{\cdot}0133$ Pa). If the backing pressure behind the nozzle is sufficient (typically $\geq 0{\cdot}5$ atm or 50 kPa), a supersonic expansion is formed. In such an expansion, the local temperature (average relative translational kinetic energy) in the centre of the gas expansion decreases rapidly with distance away from the nozzle orifice. In turn, the internal degrees of freedom of the molecular seedant gas equilibrate with the surrounding carrier gas atoms through collisions, and are hence cooled dramatically to internal temperatures of only a couple of degrees Kelvin. Under these conditions, weakly bound species held together by dispersive interactions may remain as stable species while traversing the vacuum chamber in an increasingly rarified environment.

By employing a skimmer, together with differential pumping of a second chamber, a molecular beam consisting of these stable cluster molecules entrained in the atomic carrier gas is formed. Some flexibility in the distribution of different cluster sizes formed in the beam can be attained by altering the expansion conditions (e.g. % mix of seedant in carrier gas, backing pressure, nozzle geometry and pulse duration) and by controlling with timing electronics the region of the gas pulse interrogated by the laser.

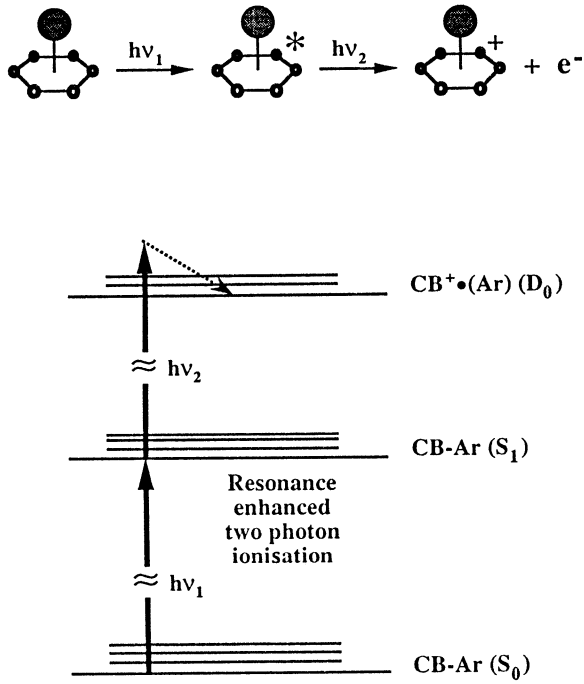


**Fig. 3.** A diagrammatic representation of the transitions involved in resonant two-photon ionisation of molecular species such as aromatic-rare gas clusters. The first photon is resonant with a vibronic transition in the neutral cluster. The second photon ionises the prepared cluster ions. In general, $h\nu_1 \neq h\nu_2$. In the present experiments however, one-colour R2PI has been used.

*(b) Resonance-enhanced Multiphoton Ionisation*

Fig. 3 illustrates the technique of resonance-enhanced multiphoton ionisation as it applies to the molecular systems that we have selected for our current experiments. The first step in the process involves the electronic excitation of the neutral cluster formed in the supersonic expansion from its ground electronic state ($S_0$), to a selected vibrational level in its first excited electronic singlet state ($S_1$). This step is carried out using doubled radiation from a tunable dye laser of a small enough bandwidth so as to ensure that a specific vibronic state of the cluster of the desired mass is electronically excited, often, but not always, to the exclusion of excitation of any other sized cluster. The subsequent step is to drive the prepared excited state of the cluster above its ionisation limit using a second photon. In this instance where two photons are sufficient to produce the ion, we refer to the technique as R2PI (resonant two-photon ionisation). The second laser photon ($h\nu_2$) may be of different wavelength from the first ($h\nu_1$), but it need not be if $2h\nu_1$ are of sufficient energy to induce ionisation. In the experiments described herein, we have used such one-colour R2PI for simplicity. Care must be taken to keep the laser power low enough to ensure that no non-resonant ionisation can occur

(i.e. ions are only formed when $h\nu_1$ is resonant with an energy level in the neutral cluster).

Scanning the wavelength of the first photon while monitoring the ion yield generated by the second photon permits the $S_1 \leftarrow S_0$ excitation spectrum of the neutral cluster to be measured. These spectra have revealed with unprecedented clarity the low frequency van der Waals vibrations of a number of aromatic–rare gas clusters that are the subject of other investigations in our laboratory (Bieske *et al.* 1989*b*, 1990*a*). Our prime interest here, however, is the spectroscopy of the cluster ion. As described below, a third laser photon is used to record the spectrum of the ionic cluster prepared using R2PI, usually with $h\nu_1$ tuned to be resonant with the $S_1(v' = 0) \leftarrow S_0(v'' = 0)$ transition.

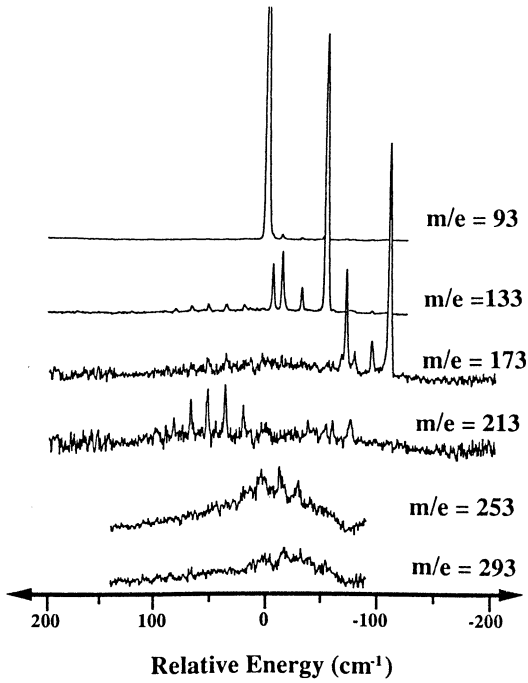


**Fig. 4.** R2PI $S_1 \leftarrow S_0$ excitation spectra of mass-selected aniline–$Ar_n$ clusters synthesised in a supersonic expansion. The identification of the cluster composition associated with each spectrum may be deduced from the *m/e* value. The upper four spectra are associated with $C_6H_5NH_2$-$Ar_n$, $n = 0$, 1, 2, 3 respectively. The lower two spectra contain significant contributions from $C_6H_5NH_2$-$Ar_n$, $n = 4$, 5 respectively, but there is some contamination of these spectra collected with the detector gate set on a particular mass due to fragmentation of higher mass clusters after ionisation giving an ion signal for the same mass fragment as that being detected directly (Bieske *et al.* 1990*d*).

### *(c) Time-of-flight Mass Spectrometry*

A distribution of cluster sizes is usually produced in a seeded supersonic expansion, e.g. for 1% benzene ($C_6H_6$) expanded in argon (1 atm) through a

1 mm nozzle, we would expect to observe significant populations of $C_6H_6$-$Ar_n$ ($n = 1, 2 \ldots 6$) clusters. Suppose our interest was in the $C_6H_6$-$Ar_2$ cluster ion. Commonly, the $S_1 \leftarrow S_0$ absorption band structure of each of the different mass neutral clusters lies in the same wavelength region and ionisation via R2PI of the cluster of the desired size is accompanied by a small amount of ionisation of other cluster sizes. Time-of-flight mass spectrometry (TOFMS) allows us to separate the spectroscopy of the individual species of clusters even if they occupy common wavelength regions. This is illustrated in Fig. 4 where we show the R2PI spectra of a series of aniline–Ar clusters ($C_6H_5NH_2$-$Ar_n$, $n = 1 \ldots 5$). Instead of monitoring the total ion current as a function of laser wavelength, the ions are accelerated down the 0·8 m flight path of a Wiley-McLaren (1955) configuration space focussing TOFMS. The arrival time at the TOFMS detector (dual tandem microchannel plates) is proportional to $(M/e)^{1/2}$, where $M$ is the cluster mass and $e$ is its charge ($e = +1$ in our experiments). Our TOFMS has a mass resolution $M/\delta M \sim 250$ at $M = 100$ amu, sufficient to discriminate easily between the different cluster species. The option of using a reflectron TOFMS is available if we need to obtain higher resolution. The output of the microchannel plates is buffered by a 100 MHz operational amplifier, displayed on a digital storage oscilloscope and sent to a dual channel boxcar averager. A gated integrator is set to monitor a small distribution of arrival times (i.e. a cluster of a specific mass) and the laser ($h\nu_1$) may then be scanned to yield the *mass-selected* R2PI spectrum.

Congestion can occur in these mass spectra due to larger clusters being formed and fragmenting to produce the smaller clusters being studied. A technique to suppress such fragment contributions has been developed recently (Bieske *et al.* 1989*a*). In this technique, ionisation by R2PI is carried out upstream from the TOF acceleration grids. Fragmentation that occurs following ionisation will produce daughter ions with altered kinetic energies and off-axis velocity components. Hence, some fragments will simply not enter the acceleration area. Those ions that enter the acceleration area are pulse extracted, by switching the high voltage extraction voltage on at a time delay, relative to the ionisation laser, that optimises the number of fragments of the mass size under study that are accelerated down the flight tube of the TOFMS, while minimising the detection of fragments that would otherwise contribute to the mass peak of interest.

The mass-selected spectra displayed in Fig. 4 demonstrate that it is possible to distinguish the spectra of clusters of different masses from each other. In contrast, if we were to measure the LIF spectrum for the same aniline–argon expansion, we would obtain a composite spectrum in which the contributions from all cluster species would be detected simultaneously, and hence overlapped. Spectral features observed in LIF spectra are therefore often difficult to associate with a cluster of a specific composition.

### *(d) Photodissociation Spectroscopy*

The binding energy of an argon atom to a benzenoid cation in the ground state is at least an order of magnitude less than the cation's electronic transition energies (~20 000 $cm^{-1}$) (Jortner *et al.* 1983). Electronically excited states of the cations we have selected for study generally display fluorescence quantum

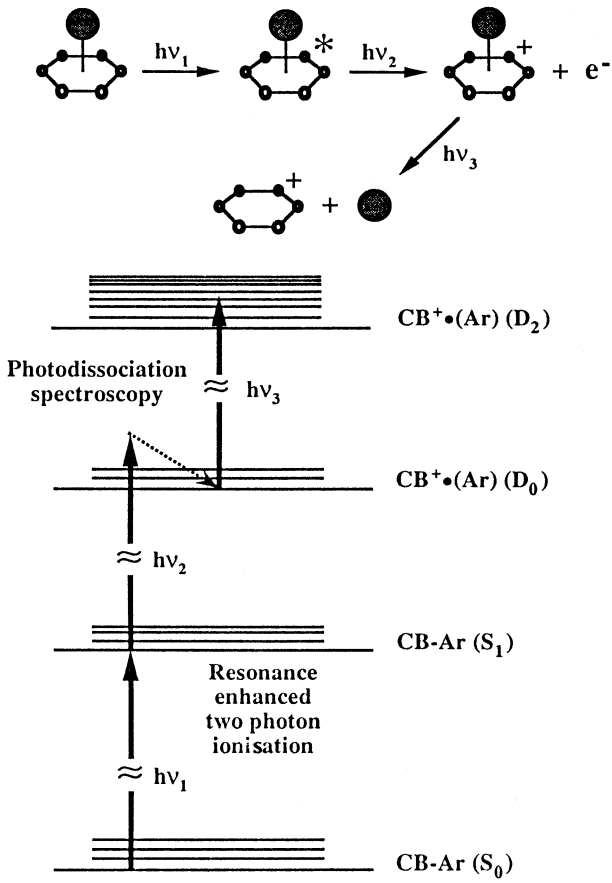


**Fig. 5.** A diagrammatic representation of the experimental procedure involved in obtaining the photodissociation spectrum of a cation complex. The first photon is resonant with a vibronic transition in the neutral cluster. The second photon ionises the prepared cluster ions. The third photon is resonant with a vibronic transition of the cation complex. The energy deposited in the excited cation complex rapidly redistributes, thus leading to dissociation of the complex and the production of a mass spectrometrically detectable parent cation.

yields substantially less than unity due to competing non-radiative processes. Hence electronic excitation of the cluster ion will result in rapid non-radiative decay (internal conversion) to highly excited vibrational levels of the ground state manifold of the cluster ion. These highly excited vibrational states are dissociative with respect to the weakly bound argon atom. Hence a transition to an internally converting electronic state will result inevitably in argon atom loss. As well, depending on the overlap of the harmonic vibrational integrals (Franck–Condon factors), radiative decay from an excited electronic level may transfer some fraction of the population to ground state levels having more vibrational energy than necessary for subsequent bond rupture. In effect, the argon atom acts a probe atom that reacts observably whenever the available

vibrational energy exceeds the bond energy. The experimental procedure that we have developed for measuring photodissociation spectra of cluster ions is illustrated in Fig. 5.

After a selected time delay, usually in the range 100–250 ns, while still in the initial acceleration region of the TOFMS, the cluster ions prepared by one-colour R2PI may be intercepted by a second dissociating laser pulse. As shown in Fig. 2, the lasers are collinear with one another and anticollinear with the molecular beam. When the probe laser photon is absorbed due to resonance with a vibronic level of the cluster ion, dissociation of the cluster ion will occur, either directly or indirectly via various routes. Scanning the dissociation laser wavelength whilst monitoring the mass-selected parent ion yield results in a photodissociation photofragment spectrum that mimics the electronic excitation spectrum of the parent cluster ion (Bieske *et al.* 1990*a*, 1990*b*). Alternatively, detection of the mass-selected cluster cations would yield an ion-dip spectrum in which a dip in ion current represents the depletion of the cation numbers due to fragmentation whenever a resonance in the cation excited state energy level is found and the cluster fragments (Tsuchiya *et al.* 1989). This latter technique has tended so far to produce poorer quality spectra in comparison with our photodissociation spectra, and has only been used in the study of neutral clusters.

There are a number of different possible processes that will result in the production of a parent cation photofragment. It is necessary to ensure that the photodissociation spectrum measured results exclusively from predissociation of the electronically excited cluster ion following one photon excitation. Care must be taken to detect this one-photon photodissociation process selectively from among all the possible production pathways of the $p$DFB$^+$ photofragment formed as a result of the two lasers intersecting the expansion of $p$DFB in argon. We list these processes:

1. $p\text{DFB}+n\text{h}\nu_1 \rightarrow p\text{DFB}^+ \quad n \geq 3$
   Multiphoton process which creates the bare cation directly. Avoid by keeping the laser power ($h\nu_1$) low.
2. $p\text{DFB}_m+nh\nu_1 \rightarrow p\text{DFB}^+ + p\text{DFB}_{m-1}$
   Ionisation and subsequent fragmentation of larger clusters due to multiphoton absorption of $h\nu_1$. Avoid by careful control of the nozzle expansion and again keeping the laser power low.
3. $(p\text{DFB})_m^+ + h\nu_2 \rightarrow p\text{DFB}^+ + p\text{DFB}_{m-1}$
   Fragmentation of larger ionised clusters on absorption of $h\nu_2$. Avoid by careful control of the nozzle expansion and using the pulse extraction technique described earlier.
4. $p\text{DFB-Ar}+2h\nu_1 \rightarrow p\text{DFB}^+ \bullet (\text{Ar})_1{}^* \rightarrow p\text{DFB}^+ + \text{Ar}$
   Creation of the ionic cluster with enough energy for immediate dissociation. Can be avoided by ensuring that the R2PI step does not have enough excess energy above the ionisation threshold to make the ionic cluster predissociative.
5. $p\text{DFB}+2h\nu_1 \rightarrow p\text{DFB}^{**} + h\nu_2 \rightarrow p\text{DFB}^+$
   Creation of a Rydberg state that is then ionised.
6. $p\text{DFB-Ar}+2h\nu_1 \rightarrow p\text{DFB}^+ \bullet (\text{Ar})_1 + h\nu_2 \rightarrow p\text{DFB}^+ + \text{Ar}$
   This is the desired process.

As well as the precautions mentioned above, a 'single' mass peak can be resolved into several discernable components separable in time due to the intrinsic delays in each of the processes (e.g. the two lasers that provide $h\nu_1$ and $h\nu_2$ are separated by a delay of 100 ns). By observing the peak behaviour when one or other of the two lasers is blocked, when altering the delay time between the two lasers, and when altering the intensities of each of the two lasers, the source of each peak can be determined, and the one of interest differentiated.

## 3. Results and Discussion

### *(a) Halobenzene•Ar Cluster Ions*

The fluorobenzene–Ar ($C_6H_5F^+\bullet(Ar)_1$ or $FB^+\bullet(Ar)_1$) and chlorobenzene–Ar ($C_6H_5Cl^+\bullet(Ar)_1$ or $CB^+\bullet(Ar)_1$) cluster ions serve as an illustrative example of various aspects of our technique of photodissociation spectroscopy. The spectra have been discussed in detail elsewhere (Bieske *et al.* 1990*a*), hence we provide only brief details here.

A one-photon molecular photodissociation spectrum represents the convolution of the molecule's absorption spectrum and an energy dependent (and possibly state-dependent) dissociation function. The simplest assumption that we can make, in order to deconvolute the photodissociation spectrum and recover the absorption spectrum, is that the dissociation probability is independent of energy. In the present case, this is probably a good assumption: fluorobenzene and chlorobenzene cations display a fluorescence quantum yield from the excited electronic state of less than $10^{-5}$ (Allan *et al.* 1977; Maier and Marthaler 1978). Thus, LIF methods are not viable to study the spectroscopy of these cations. Internal conversion is the only likely mechanism competing with radiation. In the case of the $HaB^+\bullet(Ar)_1$ cluster, rapid dissociation of the argon atom from the cluster will be the inevitable result after internal conversion to a vibrational state with more than 10 000 $cm^{-1}$ of energy. On the basis of these arguments the halobenzene cation cluster photodissociation spectra should faithfully represent their respective parent absorption spectra.

We have discussed elsewhere (Bieske *et al.* 1990*a*) how in the experiment, the dissociation process $HaB^+\bullet(Ar)_1+h\nu_2\rightarrow HaB^++Ar$ can be monitored selectively ($HaB^+$ denotes a halobenzene cation). The spectra presented in Fig. 6 extend over several thousand wavenumbers. In the lower energy regions they consist of clumps of lines, spread over 40–100 $cm^{-1}$ and separated in the lower energy regions by several hundred $cm^{-1}$. Towards higher energies the clumps begin to overlap and considerable congestion ensues. At wavelengths shorter than 455 nm, a strongly allowed, broadly structured transition becomes apparent in the $FB^+\bullet(Ar)_1$ spectrum. A similar transition dominates in the $CB^+\bullet(Ar)_1$ spectrum at wavelengths below 490 nm. Due to congestion, there do not seem to be, in either spectrum, bands that can be identified unambiguously as progressions in $HaB^+$...Ar low frequency vibrations. Hence, for these cluster ions, a determination of the $HB^+\bullet(Ar)_1$ potential surface has not been possible. Nevertheless, the spectra serve as a demonstration that the addition of a minimally perturbing adduct to a polyatomic cation permits characterisation of electronic transitions to levels that for some reason or another may not be examinable using LIF spectroscopy.

These photodissociation spectra of $CB^{+\bullet}(Ar)_1$ and $FB^{+\bullet}(Ar)_1$ assist also in the understanding of why molecular ions immersed in argon matrices have broad absorption spectra. Even for the smallest halobenzene–argon cation cluster, considerable structure accompanies each high frequency vibronic transition. It remains unclear how much of this structure is due to electronic transitions in vibrationally excited clusters, that may disappear if the ions were fully vibrationally relaxed in a matrix.

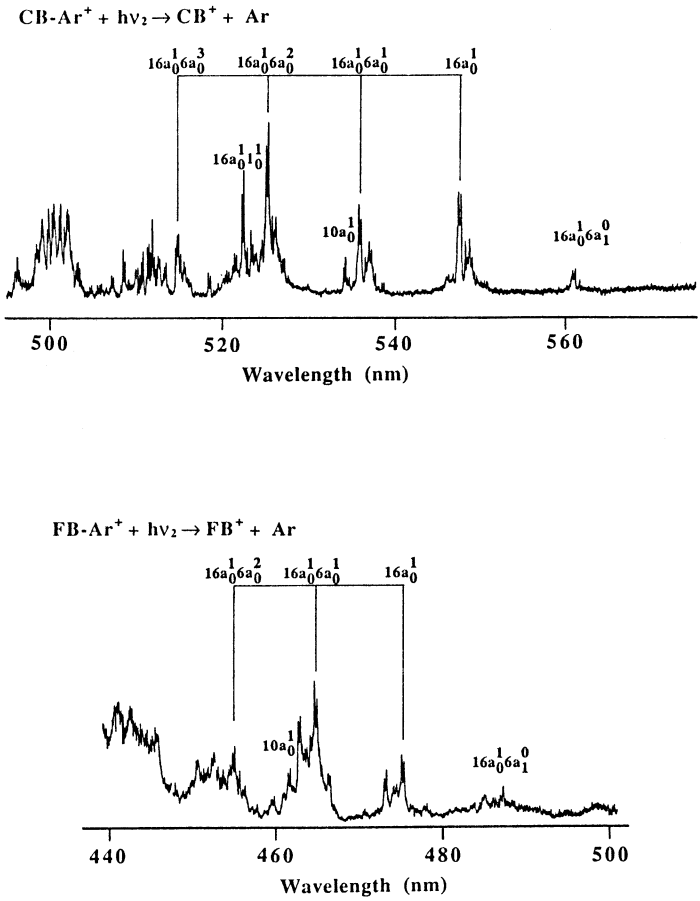


**Fig. 6.** Resonance enhanced $D_2 \leftarrow D_0$ photodissociation spectra: *top*, chlorobenzene$^{+\bullet}(Ar)_1$ cation cluster (forbidden origin ~18 087 $cm^{-1}$); *bottom*, fluorobenzene$^{+\bullet}(Ar)_1$ cation cluster (forbidden origin ~20 870 $cm^{-1}$). Relative intensities are somewhat unreliable since a number of different laser dyes were used to scan the spectral region. Assignments of major peaks are shown. Spectral resolution is ~1 $cm^{-1}$ (Bieske *et al.* 1990*a*).

### *(b) p-difluorobenzene $\bullet(Ar)_1$ and $\bullet(Ar)_2$ Cluster Ions*

We have used our experimental techniques as described above, to obtain for the first time vibrationally resolved electronic spectra of the aromatic–rare gas cluster ions *p*-difluorobenzene$^+\bullet(Ar)_1$, *p*-difluorobenzene$^+\bullet(Ar)_2$ and *p*-difluorobenzene$^+\bullet(Kr)_1$.

*p*DFB$^+$•(Ar)$_1$ cations are formed via one-colour R2PI of the neutral van der Waals cluster *p*DFB-Ar$_1$. The ionising laser (272 nm region) is tuned to be resonant with the $S_1(\upsilon' = 0) \leftarrow S_0(\upsilon'' = 0)$ electronic transition of the *p*DFB-Ar$_1$ neutral cluster. Hence the first photon ($h\nu_1$) (refer to Fig. 3) excites neutral *p*DFB-Ar$_1$ clusters to the $\upsilon = 0$ (i.e. zero quanta of vibration) level in the first excited electronic singlet state ($S_1$). A subsequent photon from this same laser ($h\nu_1$) will have sufficient energy to ionise the electronically excited neutral *p*DFB-Ar$_1$ cluster. The sum of the energies of the two absorbed photons, relative to the ionisation threshold, is such that the cation is prepared in its ground electronic state with at most 60±10 cm$^{-1}$ of excess energy, dependent on the kinetic energy of the ejected photoelectron. We have determined the location of the ionisation threshold using a two-colour resonance photoionisation measurement, where $h\nu_1$ is fixed at the energy of the *p*DFB-Ar$_1$ $S_1(\upsilon' = 0) \leftarrow S_0(\upsilon' = 0)$ band and $h\nu_2$ is scanned while the *p*DFB$^+$•(Ar)$_1$ photoion yield is being monitored.

The 60 cm$^{-1}$ of excess energy in the prepared electronic ground state of the *p*DFB$^+$•(Ar)$_1$ cluster ion is sufficient to populate the low frequency ionic cluster vibrational levels, but insufficient to excite the cation ring modes. [The lowest vibrational ring mode in *p*DFB$^+$ is $\nu_{30}'' = 144$ cm$^{-1}$ (Tsuchiya *et al.* 1989).] Thus the photodissociation spectrum obtained after one-colour R2PI preparation of the *p*DFB$^+$•(Ar)$_1$ cluster cation should be much less congested than that measured for either fluoro- or chlorobenzene$^+$•(Ar)$_1$ cation. In these latter cases, because of the relative energies of the $S_1 \leftarrow S_0$ transition of their corresponding neutral clusters and their photoionisation thresholds, the cations are prepared with excess energy after ionisation of ~1550 and ~1130 cm$^{-1}$ respectively, which is more than enough to result in excitation of many of the ring vibrational modes (Bieske *et al.* 1990*a*).

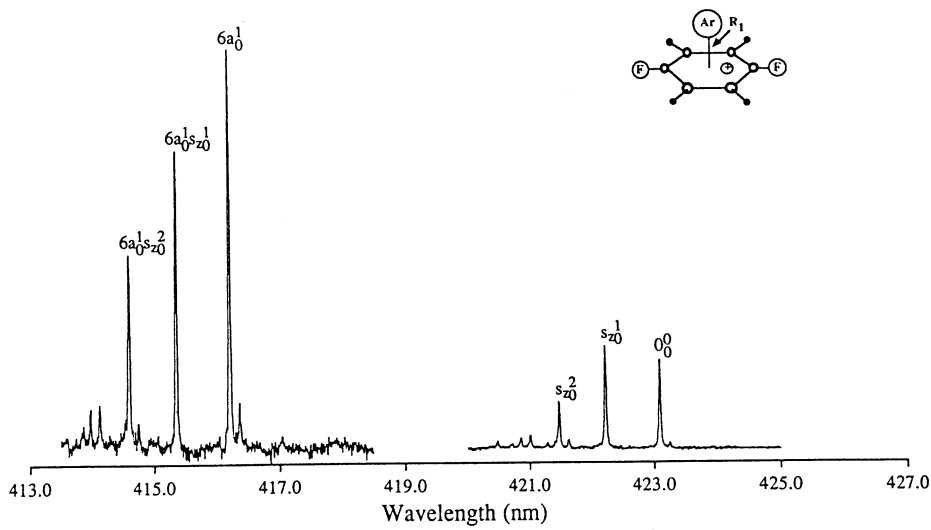


**Fig. 7.** Resonance enhanced photodissociation spectrum of the *p*DFB$^+$•(Ar)$_1$ cation cluster in the region extending from the origin $(\upsilon' = 0) \leftarrow (\upsilon'' = 0)$ of the $D_3 \leftarrow D_0$ electronic transition to the band associated with a one quantum change $(\upsilon_6' = 1) \leftarrow (\upsilon_6'' = 0)$ in the ring vibration, $\nu_6$.

The prepared ions are intercepted by a time delayed dissociating laser ($h\nu_2$), whose wavelength is scanned whilst monitoring the $p$DFB$^+$ fragment yield in the TOF mass spectrometer. This gives us a measure of the electronic excitation spectrum of the $p$DFB$^+$•(Ar)$_1$ cluster ion. Fig. 7 shows the resonance enhanced photodissociation fragment spectrum of $p$DFB$^+$•(Ar)$_1$ measured near 423 nm corresponding to the $D_3 \leftarrow D_0$ electronic transition (Bieske *et al.* 1990*b*). The spectrum displays an extended low frequency vibrational progression built on the origin with spacing ~48 cm$^{-1}$. Analysis shows that this prominent vibrational structure is probably associated with the totally symmetric stretching motion $s_z$ of the argon–aromatic cation bond (Bieske *et al.* 1990*b*). The length of the vibrational progression (i.e. several bands) indicates that this electronic transition is accompanied by substantial rearrangement of the bond between the $p$DFB$^+$ ring and the argon atom.

The measured intensity profile for the progression $s_{z0}^n$ ($n = 0,1,2$ ...) may be compared with intensities deduced from calculations of harmonic oscillator overlap integrals (Henderson *et al.* 1964) to derive an estimate for the change in the Ar...$p$DFB$^+$ equilibrium bond length ($\Delta R$) on electronic excitation of the cluster. We determine that the change in the Ar...$p$DFB$^+$ bond length upon excitation is 0·2 Å. This represents a change in the equilibrium Ar...$p$DFB$^+$ bond length upon electronic excitation larger by a factor of *three to four* than bond length changes for neutral cluster van der Waals vibrations measured to date (Yamanouchi *et al.* 1987; Weber *et al.* 1990). It would seem that the process of electronic excitation involved in the $D_3 \leftarrow D_0$ transition in the $p$DFB$^+$•(Ar)$_1$ cation influences the Ar...$p$DFB bonding more profoundly than does $S_1 \leftarrow S_0$ electronic excitation of the corresponding neutral van der Waals cluster. Detailed theoretical calculations would assist in explaining this observation. One might speculate however that the energy of the $D_3$ state of the $p$DFB$^+$•(Ar)$_1$ cation (~12 eV) is in reasonable proximity to the energies of excited electronic states of the argon atom, hence some interaction may be expected that would not be present in the corresponding neutral cluster.

The observed $p$DFB$^+$•(Ar)$_1$ cation cluster stretch frequency (~48 cm$^{-1}$) is higher than that for the corresponding neutral van der Waals cluster (41 cm$^{-1}$) (O *et al.* 1988). In the harmonic approximation, this indicates that the force constant $k = (\partial^2 V/\partial R^2)_{R=R_e}$ associated with the Ar...$p$DFB$^+$ bond is a factor of ~1·4 greater than for the Ar...$p$DFB bond in the neutral cluster. This greater bond strength in the cluster ion presumably reflects the contribution of charge-induced dipole forces to the Ar...$p$DFB$^+$ intermolecular potential.

Fig. 8 shows the resonance-enhanced photodissociation fragment spectrum of the $p$DFB$^+$•(Ar)$_2$ cluster ion (McKay *et al.* 1990). This spectrum is measured in the same way as for the mono-argon cluster ion except that the ionisation laser is tuned to coincide with the $S_1(\upsilon' = 0) \leftarrow S_0(\upsilon'' = 0)$ band in the excitation spectrum of the corresponding $p$DFB-Ar$_2$ neutral van der Waals molecule (36779 cm$^{-1}$, Knight and Kable 1988). The $p$DFB$^+$•(Ar)$_2$ cation spectrum is qualitatively similar to that for the mono-argon cluster. A progression is seen in a vibrational mode whose frequency in the excited electronic state is 44 cm$^{-1}$. Calculations carried out elsewhere (Bieske 1989) permit us to assign this frequency to the totally symmetric stretching motion ($s_{zs}$) of the two argon atoms, i.e. in which the argon atoms move in opposite directions as

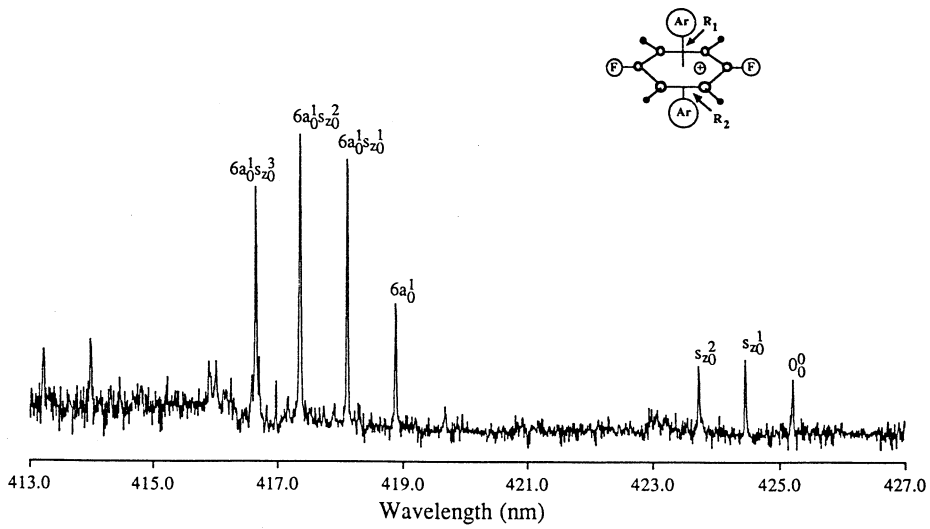


**Fig. 8.** Resonance enhanced photodissociation spectrum of the *p*DFB$^+$•(Ar)$_2$ cation cluster in the region extending from the origin ($\upsilon' = 0$)←($\upsilon'' = 0$) of the $D_3$←$D_0$ electronic transition to the band associated with a one quantum change ($\upsilon_6' = 1$)←($\upsilon_6'' = 0$) in the ring vibration, $\nu_6$.

they undergo stretching excursions away from the centre of the aromatic ring. The postulated structure of the *p*DFB$^+$•(Ar)$_2$ cluster ion is shown in Fig. 8, in which the two argons are located on opposite sides of the aromatic ring. We define a change in the coordinate associated with the symmetric stretching motion as $\Delta R = \Delta R_1 + \Delta R_2$, where $R_1$ and $R_2$ are the Ar...*p*DFB$^+$ bond lengths for each of the two argon atoms respectively. A series of relationships has been developed elsewhere for aromatic–rare gas clusters relating vibrational parameters for an (Ar)$_1$ complex to those for an (Ar)$_2$ complex (Bieske *et al.* 1990*c*). These relationships permit the intensity profile of the symmetric stretch progression of the *p*DFB$^+$•(Ar)$_2$ cluster seen in Fig. 8 to be predicted correctly from parameters deduced from the spectrum of *p*DFB$^+$•(Ar)$_1$.

From our analysis, we deduce that the change $\Delta R_1$ (or equivalently $\Delta R_2$) in the Ar...*p*DFB$^+$ bond length for *each* argon atom induced by electronic excitation is 0·1 Å, i.e. the argon atoms are both affected equivalently by electronic excitation and the magnitude of the total effect (2×(0·1 Å) = 0·2 Å) is exactly equal to that when a single argon atom is bonded to the aromatic ring. This result indicates that for the *p*DFB$^+$•(Ar)$_2$ cluster, the argon atoms behave independently of one another, i.e. the argon–argon interaction is negligible.

The $D_3$←$D_0$ photodissociation spectra shown in Figs 7 and 8 include the region involving a transition to the one-quantum vibrational state associated with the totally symmetric in-plane distortion vibration ($\nu_6$) of the *p*DFB$^+$ aromatic ring. In both *p*DFB$^+$•(Ar)$_1$ and *p*DFB$^+$•(Ar)$_2$, bands arising as a result of the low frequency vibrational motion of the Ar...*p*DFB$^+$ bond are seen built on the vibronic structure arising due to this higher frequency vibrational motion that is localised in the aromatic ring. Complete assignments of the spectroscopic structure are currently being pursued and will lead to a vibrational potential surface for *p*DFB$^+$•(Ar)$_1$ and *p*DFB$^+$•(Ar)$_2$ cations that may be compared with those for the corresponding neutral *p*DFB-Ar$_n$ clusters.

### *(c) p-difluorobenzene •Kr Cluster Ions*

Fig. 9 displays the resonance-enhanced photodissociation fragment spectrum of the $p$DFB$^+$•(Kr)$_1$ cluster ion obtained by expanding $p$DFB in a mixture of 3% krypton in helium. The spectrum is measured in a manner similar to that for the $p$DFB$^+$•(Ar)$_1$ and $p$DFB$^+$•(Ar)$_2$ cations with the exception that the ionising laser is tuned to coincide with the electronic origin of the neutral $p$DFB-Kr$_1$ van der Waals complex (36 807 cm$^{-1}$).

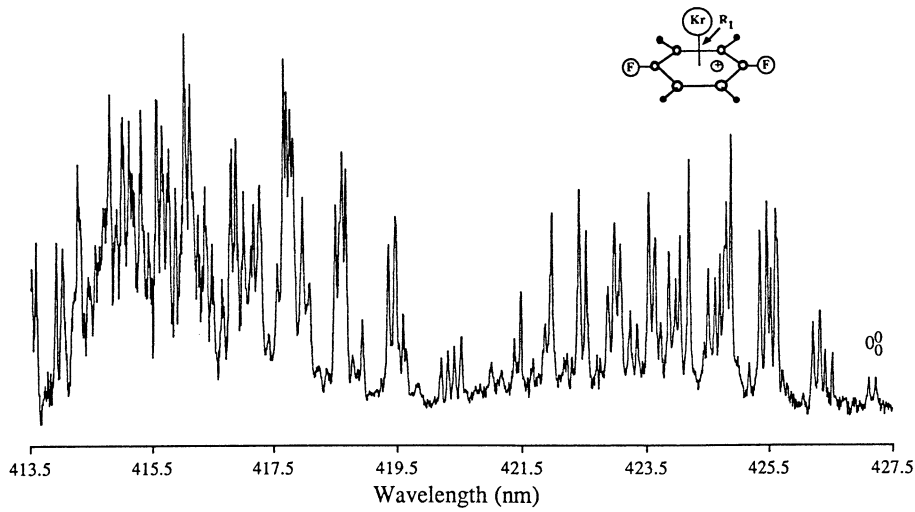


**Fig. 9.** Resonance enhanced photodissociation spectrum of the $p$DFB$^+$•(Kr)$_1$ cation cluster in the region extending from the origin ($v' = 0$)←($v'' = 0$) of the $D_3$←$D_0$ electronic transition to the band associated with a one quantum change ($v_6' = 1$)←($v_6'' = 0$) in the ring vibration, $\nu_6$.

The $p$DFB$^+$•(Kr)$_1$ spectrum is considerably more congested that its argon counterpart. Two factors are responsible for this increase in congestion. Firstly, the progressions arising due to quantum changes in the totally symmetric Kr...$p$DFB$^+$ stretching mode, $s_z$, are considerably longer than in the Ar$_1$ complex. Hence a large proportion of the bands observed correspond to transitions terminating in $D_3$ vibronic levels with much higher vibrational energy content than those observed in the Ar$_1$ cation cluster. At these higher vibrational energies, the levels associated with the cluster modes will be subject to increased contributions from anharmonic terms in the vibrational potential, hence the vibronic structure will display evidence for vibrational state-mixing. A manifestation of widespread state mixing, as has been analysed in a variety of cases in neutral polyatomic molecules (Knight 1988) is that intensity appears in many more transitions than would be the case in the absence of any state mixing.

In the $p$DFB$^+$•(Ar)$_1$ and $p$DFB$^+$•(Ar)$_2$ spectra and in the $p$DFB$^+$•(Kr)$_1$ spectrum the main source of the vibrational state mixing is stretch-bend coupling, analogous to that identified in a number of neutral aromatic–rare gas van der Waals complexes formed with argon (Bieske *et al.* 1989*b*). A detailed analysis of the coupling is currently in progress.

A second contributing factor to the increase in congestion of the $p$DFB$^+$•(Kr)$_1$ spectrum relative to that for $p$DFB$^+$•(Ar)$_1$ is a doubling of lines (and for some, an apparent quadrupling of lines). This doubling is reminiscent of a similar observation in the $D_2 \leftarrow D_0$ spectra of fluorobenzene$^+$•Ar$_1$ and chlorobenzene$^+$•Ar$_1$ cations (Bieske *et al.* 1990*a*). The source of this doubling remains open to speculation but we believe that it may be associated with spin-orbit splitting of the doublet electronic states involved in the cation electronic transitions. The splitting is absent in the spectra of all the parent cations, i.e. fluorobenzene$^+$ (Weber *et al.* 1990), chlorobenzene$^+$ (Ripoche *et al.* 1988) and *p*-difluorobenzene$^+$ (Tsuchiya *et al.* 1989). In the case of fluorobenzene$^+$- and chlorobenzene$^+$-rare gas cluster ions, the splitting has been observed for clusters formed with argon (Bieske *et al.* 1990*a*). No data are yet available for clusters with other rare gases, e.g. He, Ne, Xe. In the case of $p$DFB$^+$-rare gas clusters, the splitting is not observed for the -Ar$_1$ or -Ar$_2$ cluster ions (see Figs 7 and 8) but is observed for the -Kr$_1$ cluster. A detailed understanding of these observations must await further data for other rare gas clustering species and should lead to an improved understanding of the interaction of an aromatic cation with its 'solvent' rare gas atoms. We may however offer some general comments.

When an ion is solvated by a matrix of rare gas atoms, perturbations to the free ion electronic states usually occur. In particular, the electronic states of the isolated ion interact with matrix electronic states, resulting from promotion of an electron from the valence band to the matrix conduction band (Bondybey and Miller 1983). The disruption to the free ion spectrum will be governed in part by the energy gap between these interacting electronic states. Because of the high ionisation energy of neon (21·56 eV) compared with the energy of the lower electronic states of benzenoid cations (9–13 eV), the disruption is almost negligible for benzenoid cations solvated in neon matrices. Argon, on the other hand, has an ionisation energy much closer to the energy of these states (15·76 eV), and electronic transitions of benzenoid cations in an argon matrix suffer considerable broadening and shifting. Krypton has an even lower ionisation energy (13·99 eV), hence it may be expected to interact quite strongly with the $D_3$ state of $p$DFB$^+$ (~12 eV).

The spectra observed for the $p$DFB$^+$•(Kr)$_1$ cluster ion permit some structural information to be obtained. The progression in the totally symmetric stretching mode is complicated by the doubling of lines and by the extensive state mixing due to stretch-bend interaction. Nevertheless, an estimate of the $s_z$ frequency based on the centre of the band groups associated with the first two members of the vibrational progression gives $\nu'(s_z) = 45$ cm$^{-1}$. In the harmonic approximation, this indicates that the Kr...$p$DFB$^+$ force constant is a factor of 1·6 greater than for the Ar...$p$DFB$^+$ bond. The stronger bond found for the krypton cluster ion is as expected since the greater polarisability of krypton relative to argon will contribute to increased dispersive and ion-induced dipole terms in the intermolecular potential.

Comparison of the intensity profile with intensities deduced from calculations of harmonic oscillator overlap integrals (Henderson *et al.* 1964) as carried out for the argon cluster ions is made difficult because of the ramifications of state mixing. Each progression member is split into a clump of bands. However, we are able to obtain a reasonable estimate of the intensity profile by integrating

the intensities of members of each band group. This procedure is based on the assumption, explored in more detail elsewhere (McKay *et al.* 1990), that the intensity of each band group is likely to be derived almost exclusively from the vibronic transition moment associated with $(v' = n) \leftarrow (v'' = 0)$ progression members involving the totally symmetric stretching vibration, $s_z$. The estimate so obtained for the Kr...*p*DFB$^+$ bond length change upon electronic excitation is: $\Delta R = 0 \cdot 35$ Å. By comparison, the corresponding bond length change in the Ar...*p*DFB$^+$ cluster ion is $0 \cdot 2$ Å. We comment on this result as follows.

As mentioned above, the Kr...*p*DFB$^+$ intermolecular interaction is expected to be considerably stronger than that for Ar...*p*DFB$^+$, a consequence of the greater polarisability of krypton relative to argon. We have also referred to the lower ionisation potential of krypton ($13 \cdot 99$ eV) relative to argon ($15 \cdot 76$ eV). This latter property of krypton may be responsible for the substantially larger change in the Kr...*p*DFB$^+$ bond length, compared with that for the Ar...*p*DFB$^+$ bond length, upon electronic excitation. The closer proximity of the excited states of krypton to the *p*DFB$^+$ cation electronic states (relative to argon) will lead to stronger charge transfer and exchange interactions. As has been recognised in the spectra of polyatomic ions in rare gas matrices (Bondybey and Miller 1983), such interactions are ionic state specific, with usually stronger interaction in the excited electronic state due to its stronger electron affinity. Hence the difference in the *p*DFB$^+$...rare gas interaction upon electronic excitation is likely to be greater for krypton rather than argon. The larger bond length change for *p*DFB$^+ \bullet (Kr)_1$ relative to *p*DFB$^{+\bullet}(Ar)_1$ upon electronic excitation is consistent with these qualitative arguments.

## 4. Summary

We have employed a combination of experimental techniques, namely supersonic cooling, resonance-enhanced multiphoton ionisation, time-of-flight mass spectroscopy, and one-photon photodissociation spectroscopy, to measure vibrationally resolved electronic spectra of aromatic–rare gas cluster ions. Spectra are obtained for cation–rare gas clusters formed from the aromatic cations, fluorobenzene$^+$ ($C_6H_5F^+$), chlorobenzene$^+$ ($C_6H_5Cl^+$), bound to argon, and *p*-difluorobenzene$^+$ ($C_6H_4F_{2+}$), bound to argon and krypton. We have also obtained spectra for the *p*-difluorobenzene$^{+\bullet}(Ar)_2$cluster ion.

Analysis of the spectra reveal details concerning vibrational motion and structural changes associated with electronic excitation of the cation clusters. A theoretical model developed elsewhere for neutral clusters is found to interpret satisfactorily the trends in the data observed with changes in rare gas atom species (argon to krypton) and with increase in the number of cluster atoms, i.e. from $\bullet(Ar)_1$ to $\bullet(Ar)_2$.

This work represents one of the first comprehensive studies of the vibrationally resolved electronic spectra of aromatic–rare gas cluster ions.

## Acknowledgment

Financial support from the Australian Research Council is gratefully acknowledged.

## References


Allan, M., Maier, J. P., and Marthaler, O. (1977). *Chem. Phys.* **26**, 131.

Bieske, E. J. (1989). PhD. Thesis, Griffith University.

Bieske, E. J., Rainbird, M. W., and Knight, A. E. W. (1989*a*). *J. Chem. Phys.* **90**, 2068.

Bieske, E. J., Rainbird, M. W., Atkinson, I. M., and Knight, A. E. W. (1989*b*). *J. Chem. Phys.* **91**(2), 752.

Bieske, E. J., Rainbird, M. W., and Knight, A. E. W. (1990*a*). *J. Phys. Chem.* **94**, 3962.

Bieske, E. J., McKay, R. I., Bennett, F. R., and Knight, A. E. W. (1990*b*). *J. Chem. Phys.* **92**(7), 4620.

Bieske, E. J., Rainbird, M. W., and Knight, A. E. W. (1990*c*). *J. Chem. Phys.* (submitted).

Bieske, E. J., Rainbird, M. W., Uichanco, A. S., and Knight, A. E. W. (1990*d*). *J. Chem. Phys.* (submitted).

Blaney, B. L., and Ewing, G. E. (1976). *Ann. Rev. Phys. Chem.* **27**, 553.

Boesiger, J., and Leutwyler, S. (1986). *Chem. Phys. Lett.* **126**, 238.

Bondybey, V. E., and Miller, T. A., (1983). *In* 'Molecular Ions: Spectroscopy, Structure and Chemistry' (Eds T. A. Miller and V. E. Bondybey), p. 125 (North-Holland: Amsterdam).

Brumbaugh, D. V., Kenny, J. E., and Levy, D. H. (1983). *J. Chem. Phys.* **78**, 3415.

Butz, K. W., Catlett Jr., D. L., Ewing, G. E., Krajnovich, D., and Parmenter, C. S. (1986). *J. Phys. Chem.* **90**, 3533.

Castleman Jr., A. W., and Keesee, R. G. (1986). *Chem. Rev.* **86**, 589. See also other articles in this 'Gas Phase Clusters' edition.

DiMauro, L. F., Heaven, M., and Miller, T. A. (1984). *Chem. Phys. Lett.* **104**(6), 526.

Friedman, R. S., Kelsall, B. J., and Andrews, L. (1984). *J. Phys. Chem.* **88**, 1944.

Heaven, M., Miller, T. A., and Bondybey, V. E. (1982). *J. Chem. Phys.* **76**(7), 3831.

Henderson, J. R., Muramoto, M., and Willett, R. A. (1964). *J. Chem. Phys.* **41**, 580.

Jacobson, B. A., Humphrey, S., and Rice, S. A. (1988). *J. Chem. Phys.* **89**, 5624.

Jortner, J., Even, U., Leutwyler, S., and Berkovitch-Yellin, Z. (1983). *J. Chem. Phys.* **78**(1), 309.

Kennedy, R. A., and Miller, T. A. (1986). *J. Chem. Phys.* **85**(4), 2326.

Knight, A. E. W. (1988). *Ber. Bunsenges. Phys. Chem.* **92**, 337.

Knight, A. E. W., and Kable, S. H. (1988). *J. Chem. Phys.* **89**, 7139.

Kung, C. -Y., Miller, T. A., and Kennedy, R. A. (1988). *Phil. Trans. R. Soc. Lond.* A**324**, 223.

Levy, D. H. (1981). *Adv. Chem. Phys.* **47**, 323.

Lurito, J. T., and Andrews, L. (1985). *Chem. Phys.* **97**, 121.

McKay, R. I., Bieske, E. J., and Knight, A. E. W. (1990). (in preparation).

Maier, J. P. (1986). *J. Electron. Spectrosc.* **40**, 203.

Maier, J. P., and Marthaler, O. (1978). *Chem. Phys.* **32**, 419.

Menapace, J. A., and Bernstein, E. R. (1987). *J. Phys. Chem.* **91**, 2533.

Mons, M., Le Calve, J., Piuzzi, F., and Dimicoli, I. (1989). *J. Chem. Phys.* **92**, 2155.

O. H. K., Parmenter, C. S., and Su, M. C. (1988). *Ber. Bunsenges. Phys. Chem.* **92**, 253.

Ripoche, X., Dimicoli, I., Le Calve, J., Puizzi, F., and Botter, R. (1988). *Chem. Phys.* **124**, 305.

Tsuchiya, Y., Fujii, M., and Ito, M. (1989). *J. Chem. Phys.* **90**(12), 6965.

Turner, D. W., Baker, C., Baker, A. D., and Brundle, C. R. (1970). 'Molecular Photoelectron Spectroscopy' (Wiley-Interscience: New York).

Walter, K., Boesl, U., and Schlag, E. W. (1989). *Chem. Phys. Lett.* **162**, 261.

Weber, P. M., Buontempo, J. T., Novak, F., and Rice, S. A. (1988). *J. Chem. Phys.* **88**, 6107.

Weber, P. M., and Rice, S. A. (1988*a*). *J. Chem. Phys.* **88**, 6082.

Weber, P. M., and Rice, S. A. (1988*b*). *J. Chem. Phys.* **88**, 6120.

Weber, P. M., and Rice, S. A. (1988*c*). *J. Phys. Chem.* **92**, 5470.

Weber, Th., von Bargen, A., Riedle, E., and Neusser, H. J. (1990). *J. Chem. Phys.* **92**, 90.

Wiley, W. C., and McLaren, I. H. (1955). *Rev. Sci. Instrum.* **26**, 1150.

Yamanouchi, K., Isogai, S., Tsuchiya, S., and Kuchitsu, K. (1987). *Chem. Phys.* **116**, 123.

Yamanouchi, K., Watanabe, H., Koda, S., Tsuchiya, S., and Kuchitsu, K. (1984). *Chem. Phys. Lett.* **107**(3), 290.


Manuscript received 25 May, accepted 19 June 1990